2. Microfabrication Using X- ray Lithography

2.1 Introduction

During the last decade there has been a rapid development in microfabrication technology driven by the market need for low-cost consumer products such as portable telecommunications equipment, computers, and healthcare diagnostics. Much of the technology used for these is based on production of silicon semiconductors and microchips. Interest in non-silicon-based technologies started to grow back in the early 1980s with the development of a German fabrication process known as LIGA, an acronym for Lithography (LItho-graphie), electroplating (Galvanoformung), molding (Abformung) [1, 2]. It originated at the Karlsruhe Nuclear Research Laboratory in Germany. Since then a number of groups, mainly in Germany and the United States have been active in developing the process to make precision microcomponents for a range of innovative products such as microspectrometers, fiber–optic wave guides, micro-reactors and microfluidic devices. A few of these have been manufactured on a large scale and placed on the market. LIGA was often used to fabricate the components, which were then integrated with others into the end product. High costs are often associated with the integration and packaging of the final product.

The most active groups developing and using the LIGA process are the Sandia National Laboratories at Livermore, the Center for Advanced Microstructures and Devices (CAMD) at the Louisiana State University at Baton Rouge, in the United States, Institut fur Mikrostrukturtechnik (FZK) Karlsruhe and Antwenderzentrum BESSY, Berlin in Germany. In addition the work done in the United Kingdom at Central Microstructure Facility at the CCLRC's Rutherford Appleton Laboratory using the national synchrotron at Dares-

bury as part of a European network program has advanced fabrication techniques in mask and resist development. A small start in commercialization has been made by two companies in the United States, Axsun and International Mezzo, which provides commercial LIGA services.

Progress in commercialization has been slow owing to the absence of fast prototyping and large- scale manufacturing capabilities, and the lack of established design rules and standards. This situation was recently reviewed at a workshop at the COMS2004 conference in Edmonton. The delegates decided to form an International LIGA Interest Group to bring together major researchers, practitioners, manufacturers, and users into an international network to provide mechanisms for communication to solve the problems and be an incentive for commercialization.

Since 1980 numerous reports and papers on the development and use of the LIGA process have been published and are too numerous to be listed here. A more recent overview of the current status of this process was given by Hruby at the HARMST Conference in 2003 [3], and commercialization issues were reviewed recently by Tolfree at COMS2004 [4] and Goettert at COMS2004 [5].

The latest market survey [6] indicated that a global market valued in excess $40 billion is emerging for microproducts. The increased interest in nanotechnology driven by the prospect of producing new non-silicon-based materials with unique properties, has increased market estimates to over a $1trillion. Micro-nanomanufacturing is now a key value-added element in many sectors of industry.

The boundaries between nanotechnology and microtechnology may be blurred, but there is a degree of commonality in the techniques and equipment involved in both - but they are, in essence and in application, very different. It is at the nano not the micro scale that the physical and chemical properties of materials change. Microfabrication is essentially a top-down technology but at the nanoscale, either top-down or bottom-up techniques can be used, and the latter are significantly different. Many products require a variety of top-down processes for their manufacture. For example, the common CD has data pits about 500 nm wide and 125 nm deep formed

in a plastic disc. The read-write heads are very precise mechanisms that require a number of electro- mechanical processes.

Extensive papers and reviews on microfabrication technologies have been published. Two examples are: "The Fundamentals of Microfabrication" by Madou 2002 [7], and 'Microfabrication using Synchrotron Radiation" by Tolfree in 1998 [8]. These and others can be found in the literature and on internet sites, cover most of the relevant principles and issues associated with the development and exploitation of the technologies. It was therefore decided to restrict the content on this chapter to microfabrication using lithographic X-ray techniques. This technique is known as deep X- ray lithography (DXRL), is like all lithographic processes, ultimately limited in line-width by the wavelength of the illuminating radiation. The conversion from a 2-D pattern to a 3-D structure is dependent on a number of factors, which are examined below.

There are multiple types of lithography, including UV, deep UV, X- ray and electron-beam lithography. Currently, for non-silicon-based materials, the highest precision can be achieved using DXRL with very parallel, high-energy x- rays from a synchrotron radiation source (SRS). It is the increased access provided by the large number (>80) of synchrotrons now operating world wide, coupled to availability of low-solubility resists, thus reducing exposure time that has encouraged a greater interest in DXRL. This technique still has to find a wider community of users outside of research but it will have a significant role to play in the range of tools and processes required to develop a micro-nanotechnology (MNT)-based industry.

Micro-nanotechnology (MNT) is pervasive and will have an impact, sometimes disruptive, on almost every industry sector and through the generation of new products and systems, on the society in general. The universal use of the mobile telephone and ink-jet printer are two well-known examples. The availability of a vast range of new consumer and industrial products such as sensors, embedded transducers and actuators, displays, health care diagnostics etc. will revolutionize the way people will live and work in the future.

2.2 X- ray Lithography

2.2.1. History

International Business Machines (IBM) first combined electrodeposition and x- ray lithography in 1969. They made high-aspect ratio metal structures by plating gold patterns of 20 μm in thickness in a resist that had been exposed to x- rays. The IBM work was an extension of through-mask plating, also pioneered by IBM in 1969, and was directed toward the fabrication of thin film magnetic recording heads. A historical background of lithography was provided by Cerrina [9].

The development of the LIGA process referred to above required small slotted nozzles for uranium isotope separation [10] to be produced. Since then, the X- ray lithographic technique has been developed to fabricate a variety of microstructures in materials [11 - 19]. The potential of LIGA for the development of microsystems was reviewed by Bacher [20]. Essentially, a three-step process, the LIGA technique can be used to make 3D microstructures.

By adding molding techniques the broader implications of x- ray lithography as a means of low-cost manufacturing of a wide variety of microparts with unprecedented accuracy from various materials can be realised. In Germany, x- ray lithography was originally developed outside of the semiconductor industry.

Early pioneering work in the use of synchrotron radiation for microfabrication was carried out by Professor Guckel at the University of Wisconsin in the United States. This included use of the LIGA technique to develop micromotors [21-24]. Guckel repositioned the field in light of semiconductor process capabilities and brought it closer to standard manufacturing processes.

2.3 Synchrotron Radiation (SR)

2.3. General Characteristics

The radiation emitted by relativistic electrons when traversing a magnetic field can be understood from purely classical electromagnetic theory. Its properties can be expressed by basic equations that are used in the design of synchrotron radiation sources [25-32]. A basic introduction to synchrotron radiation sources is given by Marks [33] and a general review that provides details on the subject by Turner [34]. The power of the emitted radiation is inversely proportional to the mass of the charged particle, so electrons yield useful quantities of radiation in the visible and X- ray regions of the electromagnetic spectrum.

Centripetal acceleration of highly relativistic charged particles in a magnetic bending field results in the tangential emission of synchrotron radiation over a wide spectrum at every point of the curved particle trajectory. Considering only electrons, the emission pattern is essentially determined by that of a single circulating electron.

With reference to Fig. 2.1, the radiation pattern emitted by relativistic electrons can be transformed into the laboratory reference frame, resulting in its being compressed in a narrow forward cone, tangential with respect to the electrons' circular path. This natural collimation is an important characteristic property of synchrotron radiation. As the electron beam sweeps out the curved path, a continuous fan of radiation results in the horizontal plane while the distribution in the vertical plane is highly collimated.

The opening half-angle of the emission cone of radiation is wavelength-dependent [35], its angular distribution can be approximated by a Gaussian distribution, the width of which is related to the kinetic energy, E, and the rest energy (mc^2). The natural divergence δ_n is given by:

$$\delta_n = (mc^2)/E \tag{2.1}$$

The divergence is an important parameter when considering the use of synchrotron radiation sources for deep x- ray lithography. This has to be as low as possible but is limited to the practical values obtainable for E, which are in the range (1.5-3) GeV for typical national sources, resulting in values for the natural divergence between 0.2 and 0.3 mrad in the x- ray region.

The continuous emission of radiation excites particle oscillations that give rise to a finite extension of the particle beam and corresponding angular deviations with respect to the ideal trajectory. Since the direction of photon emission follows the instantaneous particle direction, an additional angular width, δ_p, results, which is independent of the natural divergence and when added to the natural divergence it forms the total angular width of the synchrotron radiation and is given by:

$$s_{tot} = (\delta n^2 + \delta p^2)^{1/2} \tag{2.2}$$

The electron beam emittance is determined by the particular design of the synchrotron but can be optimized to be similar in magnitude to the natural divergence. A typical value for s_{tot} is in the range 0.3-0.4 mrad that leads to a vertical intensity distribution of the beam. At a distance of 10 m from the emission point and with a typical beam width of 3-4 mm, the beam is seen as a broad radiation fan in the horizontal direction. In calculating the above, the finite width of the beam has been ignored but could be important at the location of the lithography station on an external beam line on a synchrotron. When the beam width is taken into account, the product of beam size, W, and its angular width, δ_t, is given by the emittance, E:

$$E = W\delta_t \tag{2.3}$$

2.3.2 Spectral Characteristics

Owing to both longitudinal and transverse oscillations of the circulating electrons, individual components in the frequency spectrum become smeared out, resulting in a continuous spectrum of radiation

being emitted from the infra-red to wavelengths shorter than a critical wavelength, λ_c, in the hard x- ray region.

The spectrum shape is characterized by the electron energy, the beam current and the magnetic field in the accelerator [36]. The spectral distribution from a small elemental arc of radius, R, along the electron orbit can be described in terms of a critical wavelength, λ_c, Angstrom.

$$\lambda_c = 18.6/BE^2 \tag{2.4}$$

Where E is the electron energy (GeV), B is the bending field (Tesla). The critical wavelength is a useful parameter for characterising emission. It represents the value of wavelength that equally divides the total integrated photon energy. Since the spectrum extends into long wavelengths and the photon energy is inversely proportional to wavelength, the critical wavelength is near the short wavelength end of the spectrum. A typical spectrum from a dipole magnet in which the emission is integrated over the complete fan of radiation is shown in Fig. 2.1. For a source of fixed radius, the radiated power varies as the fourth power of the electron energy.

2.3.3 Spectral Brilliance and Brightness

The finite size of the electron beam and the correlation between individual electrons and their orbits is characterized by phase space distributions.

The photon flux radiated by the source can be described by a number of different parameters. The spectral flux is the number of photons/s/mrad horizontal emitted into a 0.1% bandwidth, the emission being integrated fully in the vertical plane.

The brightness is the spectral flux per mrad vertical; it therefore has units of photons/s/mrad^2 per 0.1% bandwidth. Where the incident beam is focused on a sample, and the source area becomes important, the concept of brilliance, the brightness per unit source area, is used. This has units of photons/s/mrad^2/mm^2 per 0.1% bandwidth.

The value of brightness or brilliance for any particular synchrotron is dependent on the design of the accelerator and particularly its magnet lattice, a high value of brilliance being required for good resolution [37]. The quality of the radiation source is therefore characterized by its spectral brilliance and the spectral distribution of the emission.

Brightness can be increased by the use of insertion devices such as wigglers and undulators, placed in straight sections of the storage ring. These devices have a periodic magnetic structure and therefore produce an oscillatory path of the electrons with enhancement and modification of the radiation. The theory associated with these devices is given in [38,39].

The enhanced penetrating power and beam intensity of the higher energy X- rays resulting from the use of wigglers enables the production of deeper molds, thus facilitating the manufacture of 3D microstructures. Using data from the Daresbury synchrotron source, parameters required for deep lithography using wiggler radiation were calculated by using software developed at Daresbury Laboratory in the United Kingdom.

It should be noted that a beryllium window can withstand a 1 atmosphere pressure differential across a small diameter (<1 inch). For large area exposures, windows up to 6 cm in diameter have been developed. Beryllium windows age with x- ray exposure and must be replaced periodically. This is one of the limitations of using external X- ray beams and adds to the overall operational cost.

2.4 Microfabrication Process

2.4.1 General

An overview of microlithography, micromachining, and microfabrication has been given in a SPIE Handbook [9]. Methods exist for fabricating microstructures but the use of deep X- ray lithography and the LIGA process referred to above provides the highest dimension precision.

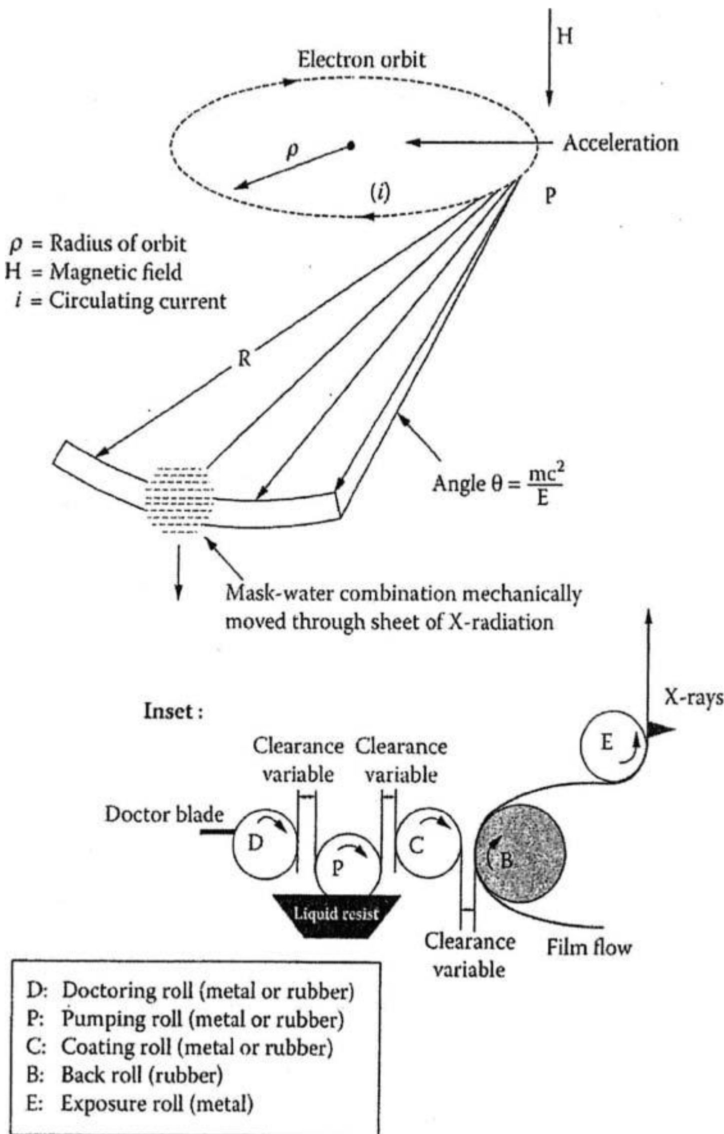

Fig. 2.1. Schematic of an x- ray exposure station with a synchrotron radiation source. The x- ray radiation opening angle, θ, is tangential to the path of the electron describing a line on an intersecting substrate. (M. Madou, "Fundamentals of Microfabrication", 2nd edition, 2002, CRC Press [7])

However, limitations in the materials that can be used and the relatively high cost of the process from prototyping to large-scale manufacture of components has restricted it wider use. The development of new resists, (SU8) increased knowledge of the process, and the wider availability of synchrotron storage rings has awakened renewed interest in LIGA as a viable process technology. The current support for nanotechnology has also raised questions about the boundaries that can be reached for top-down processing.

2.4.2 LIGA Process

LIGA is a three-step process (Fig. 2.2). Although here, we consider x- ray based lithography, UV-LIGA and Laser-LIGA techniques have also reached an advanced stage of development. UV–LIGA in particular has encouraged the production of a negative resist known as SU-8 that can also be used in X- ray lithography owing to its increased radiation sensitivity over more commonly used polymethylmethacrylate (PMMA) resists, thus reducing exposure time and subsequent costs.

The penetrating power of X- rays compared to other longer wavelength radiations allows the fabrication of structures that have vertical dimensions from hundreds of microns to millimeters and horizontal dimensions as small as microns. These 3-D microstructures with high aspect ratios offer a range of microcomponents for many useful applications.

2.4.3 Lithography Steps

The first step using x- ray lithography involves exposing a thick layer of resist through a patterned mask .to a high-energy beam of x-rays from a synchrotron. The pattern is etched into the resist substrate by the use of x- rays. A chemical solvent is used to dissolve away the damaged material, resulting in a negative relief replica of the mask pattern. Certain metals can be electrodeposited into the re-

sist mold. After removal of the resist, a freestanding metal structure is produced. The metal structure may be a final product, or serve as a mold insert for precision plastic molding. Molded plastic parts may then be final products or lost molds. The plastic mold retains the same shape, size, and form as the original resist structure but is produced quickly. The plastic lost mold may subsequently metal parts in a secondary process, or generate ceramic parts using a slip casting process.

2.4.4 X- ray Lithography

X- ray lithography is basically a shadow printing process in which patterns coated on a mask are transferred into a third dimension in a resist material, normally PMMA. This is subsequently chemical process to dissolve away the volume of material damaged by the x-rays. The quality of the remaining structure is dependent on the beam exposure, the precision of patterning on the mask and the purity and processing of the resist material. Beyond exposure it is the precision of electroforming and micromolding processes that determines the quality of the final product.

Micromachining techniques are changing manufacturing approaches for a wide variety of small parts. Frequently, semiconductor batch microfabrication methods are considered along with traditional serial machining methods. In this sense, x- ray lithography and pseudo x- ray lithography processes are classed as hybrid technologies, bridging semiconductor and classical manufacturing technologies. The ability of x- ray lithography and pseudo x- ray lithography for creating a wide variety of shapes from different materials makes these methods similar to classical machining, with the added benefit of high aspect ratios and absolute tolerances that are possible using lithography and other high-precision mold fabrication techniques.

2.4.5 X- ray Masks

Good quality, radiation resistant masks are an essential element in lithography. To be highly transmissive to x- rays, the mask substrate must be a low-Z (atomic number) thin membrane.

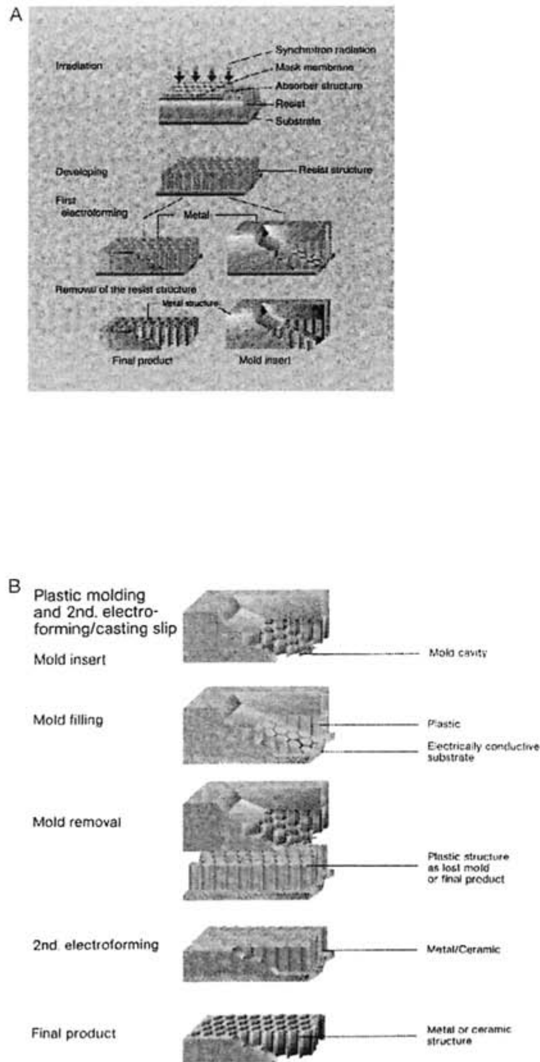

Fig. 2.2. (A) Basic x- ray exposure: (1) x- ray deep-etch lithography and, (2) primary electroforming process. (B) Plastic molding and secondary electroforming process. (From Lehr and Schmidt, "The LiGA Technique", IMM GmbH, Mainz-Hechstein, 1995)

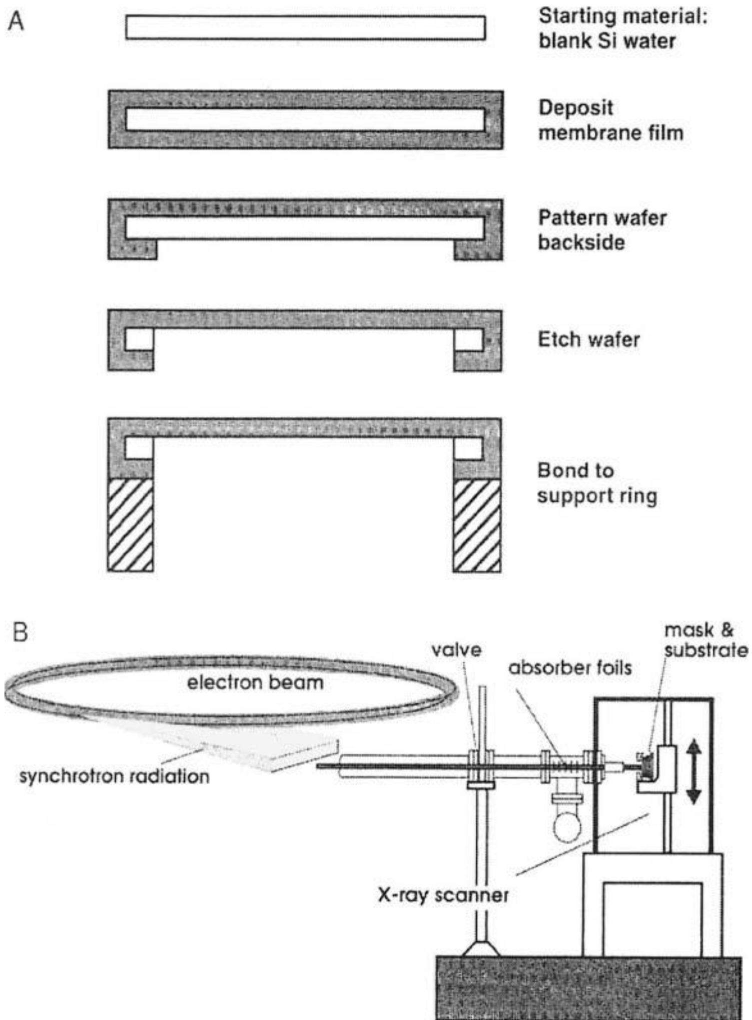

Fig. 2.3. Schematic of a typical x- ray mask (A) and mask and substrate assembly in an x- ray scanner (B). (From M. Madou, "Fundamentals of Microfabrication", 2nd Edition, 2002, CRC Press [7])

Table 2.1. Comparison of masks for use in x- ray lithography and the semiconductor industry.

Feature	**Semiconductor lithography**	**X- ray lithography**
Transparency	≥50%	≥80%
Absorber thickness	±1 μm	10 μm or higher
Field size	50 x 50 mm^2	100 x 100 mm^2
Radiation resistance	= 1	= 100
Surface roughness	<0.1 μm	<0.5 μm
Waviness	<±1 μm	<±1 μm
Dimensional stability	<0.05 μm	<0.1-0.3 μm
Residual membrane stress	~10^8 Pa	~10^8 Pa

X- ray masks should withstand many exposures without distortion, must be aligned with respect to the sample, and must be rugged. Possible x- ray mask architecture and its assembly with a substrate in an x- ray scanner are shown in Fig. 2.3. The mask shown here has three major components: an absorber, a membrane or mask blank, and a frame. The absorber contains the information to be imaged onto the resist. It is composed of a material with a high atomic number (Z),; often gold is used that is patterned to a membrane material with a low Z. The high-Z material absorbs x- rays, whereas the low-Z material transmits x- rays.

The frame is robust in relation to the membrane/absorber assembly so that the whole can be handled. The requirements for x- ray masks in x- ray lithography differ substantially from those for the semiconductor industry. A comparison is presented in Table 2.1.

The main difference lies in the thickness of the absorber. To achieve high contrast, a very thick absorber (>10 μm vs. 1 μm) and highly transparent mask blanks (transparency >80%) must be used because of the low resist sensitivity and the great depth of the resist. Another difference focuses on the radiation stability of membrane and absorber. For conventional optical lithography, the supporting substrate is a relatively thick, optically flat piece of glass or quartz highly transparent to optical wavelengths. It provides a highly stable (>10^6 μm) basis for the thin (0.1 μm) chrome absorber pattern. In contrast, the x- ray mask consists of a very thin membrane (2 to 4 μm) of low-Z material carrying a high-Z thick absorber pattern. A single exposure in x- ray lithography results in an exposure dose 100 times higher than in the semiconductor case.

2.4.6 Mask Materials

The low-Z membrane material in an x- ray mask must have a transparency for rays with a critical wavelength, λ_c, from 0.2 to 0.6 nm of at least 80% and should not scatter those rays. To avoid pattern distortion, the residual stress, σ_r, in the membrane should be less than 10^6 N/m^2. Mechanical stress in the absorber pattern can cause in-plane distortion of the supporting thin membrane, requiring a high Young's modulus for the membrane material. During one typical lithography step, the masks may be exposed to 1 MJ/cm^2 of x- rays. Since most membranes must be very thin for optimal transparency, a compromise has to be found among transparency, strength, and form stability. Important x- ray membrane materials are listed in Table 2.2. The higher radiation dose in x- ray lithography prevents the use of BN and compound mask blanks that incorporate a polyimide layer. Those mask blanks are perfectly appropriate for classical semiconductor lithography work but will not do for x- ray lithography processes. Mask blanks of metals such as titanium (Ti) and beryllium were specifically developed for x- ray lithography applications because of their resistance to radiation breakdown. In comparing titanium and beryllium membranes, beryllium can have a much greater membrane thickness, d, and still be adequately trans-

parent. For example, a membrane transparency of 80%, essential for adequate exposure of a 500 μm thick PMMA resist layer, is obtained with a thin 2 μm titanium film, whereas, with beryllium, a thick 300 μm membrane achieves the same result. The thicker beryllium membrane permits easier processing and handling. In addition, beryllium has a greater Young's modulus E than titanium and, since it is the product of E and d that determines the amount of mask distortion, distortions due to absorber stress should be much smaller for beryllium blanks. Beryllium is an excellent membrane material for x- ray lithography because of its high transparency and excellent damage resistance. Stoichiometric silicon nitride (Si_3N_4) used in x-ray mask membranes may contain numerous oxygen impurities, absorbing x- rays and thus producing heat. This heat often suffices to prevent the use of nitride as a good x- ray lithography mask. Single-crystal silicon masks have been made (1 cm square and 0.4 μm thick, and 10 cm square and 2.5 μm thick) by electro-chemical etching techniques. For Si and Si_3N_4, Young's modulus is quite low compared with CVD-grown diamond and SiC films, with a Young's modulus as high as three times. Higher stiffness materials are more desirable, because the internal stresses of the absorbers, which can distort mask patterns, are less of an issue. Unfortunately, diamond and SiC membranes are also the most difficult to produce.

Table 2.2. Comparison of membrane materials for x- ray masks

Material	X- ray transparency	Observations
Silicon	0 (50% transmission at 5.5 μm thickness).	Single-crystal silicon, stacking faults cause scattering to occur, material is brittle.
SiC	0 (50% transmission at 2.3 μm thickness).	Amorphous with resistance to fracture.
Diamond	0 (50% transmission at 4.6 μm thickness).	High stiffness and transparency

The requirements on the absorber are high attenuation (>10 dB), stability under radiation over an extended period of time, negligible distortion, ease of patterning, and low microstructural defect density. Typical absorber materials are listed in Table 2.3. Gold is used most commonly; tungsten and other materials are used infrequently. In the semiconductor industry, an absorber thickness of 0.5 μm might be sufficient, whereas x- ray lithography deals with thicker layers of resist, requiring a thicker absorber material to maintain the same resolution.

Table 2.3. Comparison of absorber materials for x- ray masks

Material	Observations
Gold	Not the best stability (grain growth), low stress, electroplating only, defects repairable (thermal exp coefficient 14.2°C^{-1} 10^{-6}) (0.7 μm for 10 dB).
Tungsten	Refractory and stable, special care is needed for stress control, dry etchable, repairable (thermal exp coefficient 4.5°C^{-1} 10^{-6}) (0.8 μm for 10 dB).
Tantalum	Refractory and stable, special care is needed for stress control, dry etchable, repairable.
Alloys	Easier stress control, greater thickness needed to obtain 10 dB.

Figure 2.4 illustrates how x- rays, with a characteristic wavelength of 0.55 nm, are absorbed along their trajectory through a Kapton pre-absorber filter, an x- ray mask, and resist. The low-energy portion of the synchrotron radiation is absorbed mainly in the top portion of the resist layer, since absorption increases with increasing wavelength. The Kapton pre-absorber filters out much of the low-energy radiation to prevent over exposure of the top surface of the resist. The x- ray dose at which the resist gets damaged, D_{dm}, and the dose required for development of the resist, D_{dv}, as well as the

"threshold dose" at which the resist starts dissolving in a developer, D_{th}, are all indicated in Fig. 2.4. In the areas under the absorber pattern of the x- ray mask, the absorbed dose must stay below the threshold dose, D_{th}. Otherwise, the structures partly dissolve, resulting in poor feature definition. From Fig. 2.4, we can deduce that the height of the gold absorbers must exceed 6 μm to reduce the absorbed radiation dose of the resist under the gold pattern to below the threshold dose, D_{th}. In Fig. 2.5, the necessary thickness of the gold absorber patterns of an x- ray mask is plotted as a function of the thickness of the resist to be patterned; the Au must be thicker for thicker resist layers and for shorter characteristic wavelengths, λ_c, of the x- ray radiation. To pattern a 500 mm high structure with a λ_c of 0.225 nm, the gold absorber must be more than 11 μm in height.

Exposure of more extreme photoresist thickness requires x- ray photon energies that are significantly higher. At 3000 eV, the absorption length in PMMA roughly measures 100 μm, which enables the above-mentioned 500 μm exposure depth. Using 20,000 eV photons results in absorption lengths of 1 cm. PMMA structures up to 10 cm thick have been exposed this way. A high-energy mask for high-energy exposures has a gold absorber 50 μm thick and a blank membrane of 400 μm thickness of silicon. An absorption contrast of 400 when exposing a 1000 μm thick PMMA sheet can be obtained. An advantage of using such thick silicon blank membranes is that larger resist areas can be exposed, since it does not depend on a fragile membrane-absorber combination.

2.4.7 Single-layer Absorber Fabrication

To make a mask with gold absorber structures of a height above 10 μm, one must first succeed in structuring a resist of that thickness. The height of the resist should be higher than the absorber itself so as to accommodate the electrodeposited metal in between the resist features. Currently, no means to structure a resist of that height with sufficient accuracy and perfect verticality of the walls exists, unless x- rays are used.

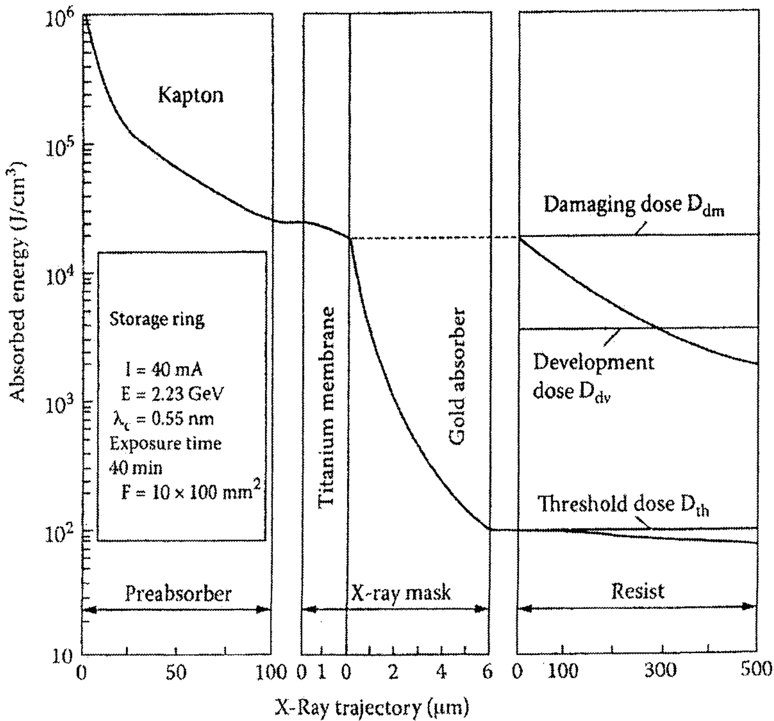

Fig. 2.4. Absorbed energy along the x- ray trajectory including a 500 μ m thick PMMA specimen, x- ray mask, and a Kapton pre-absorber. (From P. Bley, W. Menz, W. Bacher, K. Feit, M. Harmening, H. Hein, J. Mohr, W. Schomberg and K. Stark, "Application of the LiGA Process in the Fabrication of 3-D Structures", 4th International Symposium on Microprocess Conference, Japan, 1991, p.p. 384-389)

Different procedures for producing x- ray masks with thicker absorber layers using a two-stage lithography process have been developed. First, an intermediate mask is made with photo or electron-beam lithography. This intermediate mask starts with a 3 μ m thick resist layer, in which case the needed line-width accuracy and photoresist wall steepness of printed features are achievable. After gold plating in between the resist features and stripping of the resist, this intermediate mask is used to write a pattern with x- rays in a thicker resist, say 20 μ m thick. After electrodepositing and resist stripping, the actual x- ray mask (that is, the master mask) is obtained.

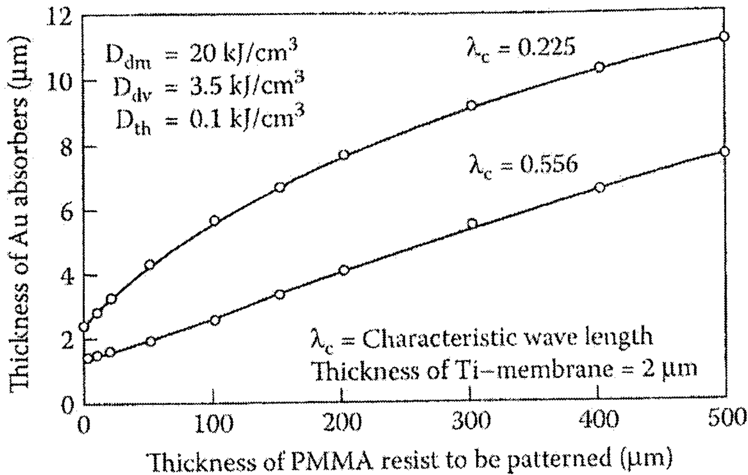

Fig. 2.5. Minimum thickness of gold absorbers used for the x- ray mask. (From P. Bley, W. Menz, W. Bacher, K. Feit, M. Harmening, H. Hein, J. Mohr, W. Schomberg and K. Stark, "Application of the LiGA Process in the Fabrication of 3-D Structures", 4th International Symposium on Microprocess Conference, Japan, 1991, p.p. 384-389)

Since hardly any accuracy is lost in the copying of the intermediate mask with x- rays to obtain the master mask, it is the intermediate mask quality that determines the ultimate quality of the x- ray lithographic-produced microstructures. The structuring of the resist in the intermediate mask is handled with optical techniques when the requirements of the x- ray lithography structures are less stringent. The minimal lateral dimensions for optical lithography in a 3 μm thick resist typically measure about 2.5 μm. Under optimal conditions, a wall angle of 88° is achievable. With electron beam lithography, a minimum lateral dimension of less than 1 μm is feasible. The most accurate pattern transfer is achieved through reactive ion etching of a tri-level resist system. In this approach, a 3 to 4 μm thick polyimide resist is first coated to the titanium or beryllium membrane, followed by a coat of 10 to 15 nm titanium deposited with magnetron sputtering. The thin layer of titanium is an excellent

etch mask for the polyimide; in the optimized oxygen plasma, the titanium etches 300 times slower than the polyimide. To structure the thin titanium layer itself, a 0.1 μm thick optical resist is used. Since this top resist layer is so thin, excellent lateral tolerances result. The thin Ti layer is patterned with optical photolithography and etched in the argon plasma. After the thin titanium layer is etched, exposing the polyimide locally, an oxygen plasma helps to structure the polyimide down to the titanium or beryllium membrane. Lateral dimensions of 0.3 μm can be obtained in this fashion. Patterning the top resist layer with an electron beam increases the accuracy of the three-level resist method even further. Electrodeposition of gold on the titanium or beryllium membrane and stripping of the resist finishes the process of making the intermediate x-ray lithography mask. To make a master mask, this intermediate mask is printed by x- ray radiation onto a PMMA-resist-coated master mask. The PMMA thickness corresponds to a bit more than the desired absorber thickness. Since the resist layer thickness is in the 10 to 20 μm range, a synchrotron x- ray wavelength of 0.1 nm is adequate for the making of the master mask. A further improvement in x- ray lithography mask making is to fabricate intermediate and master mask on the same substrate, greatly reducing the risk for deviations in dimensions caused, for example, by temperature variations during printing.

2.4. Alignment of X- ray Mask to Substrate

The mask and resist-coated substrate must be properly registered to each other before they are put in an x- ray scanner. Alignment of an x- ray mask to the substrate is a problem, since no visible light can pass through most x- ray membranes. To solve this problem windows are etched in a titanium x- ray membrane. Diamond membranes have a potential advantage here, as they are optically transparent and enable easy alignment for multiple irradiations without a need for etched holes.

Figure 2.6 illustrates an alternative, x- ray alignment system involving capacitive pickup between conductive metal fingers on the mask and ridges on a small substrate area; Silicon in this case (U.S.

Patent 4,607,213 [Registered in 1986] and 4,654,581 [Registered in 1987]). When using multiple groups of ridges and fingers, two axis lateral and rotational alignment become possible.

Another alternative may involve liquid nitrogen-cooled Si (Li) x-ray diodes as alignment detectors, eliminating the need for observation with visible light. A procedure has been developed to eliminate the need for an x- ray mask membrane. Unlike conventional masks, the so-called x- ray transfer mask does not treat a mask as an independent unit. The technique is based on forming an absorber pattern directly on the resist surface forming a conformal, self-aligned, or transfer mask. An example process is shown in Fig. 2.7. In this sequence, a transfer mask plating base is first prepared on the PMMA substrate plate by evaporating 0.7 nm of chromium (as adhesion layer) followed by 50 nm of gold using an electron beam evaporator.

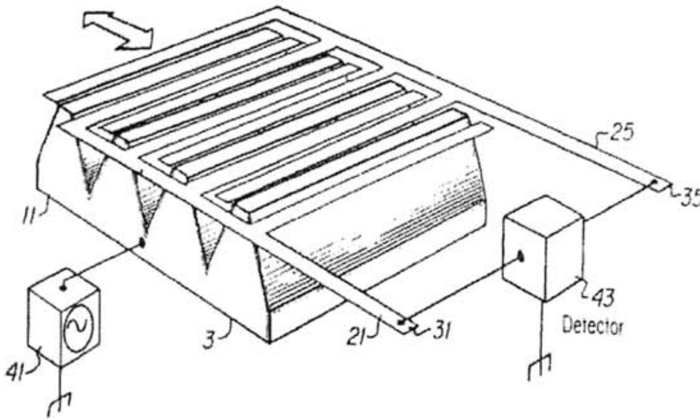

Fig. 2.6. Mask alignment system in x- ray lithography. Invention described by U.S. Patents 4,654,581 (Registered in 1987) and 4,607,213 (Registered in 1986)

A 3 µm thick layer of standard Novolak-based resist is then applied over the plating base and exposed in contact mode through an optical mask using an ultraviolet exposure station. Three microme-

ters of electroplated gold on the exposed plating base further completes the transfer mask.

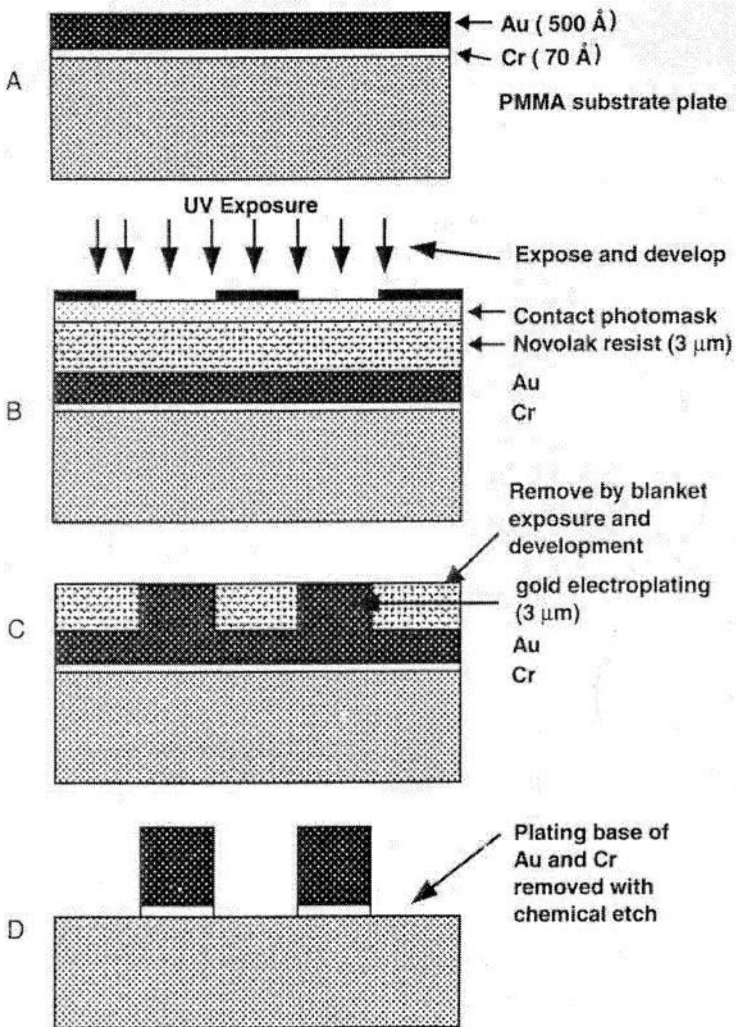

Fig. 2.7. Sample transfer mask formation. (From M. Madou, 'Fundamentals of Microfabrication', 2nd edition, 2002, CRC Press [7])

A blanket exposure and subsequent development remove the remaining resist. The 50 nm of Au plating base is dissolved by a dip of 20 to 30 s in a solution of potassium iodide (5%) and iodine (1.25%) in water; the Cr adhesion layer is removed by a standard chromium etch.

Fabrication of the transfer mask can thus be performed using standard lithography equipment available at almost any lithography shop. Depending on the resolution required, the x- ray transfer mask can be fabricated using known photon, electron beam, or x- ray lithography techniques. The patterning of the PMMA resist with a self-aligned mask is accomplished in multiple steps of exposure and development.

An example of a cylindrical resonator made this way is shown in Fig. 2.8. Each exposure/development step involves an exposure dose of about 8 to 12 J/cm^2. Subsequent 5-min development steps remove ~30 μm of PMMA. In seven steps, a self-supporting 1.5 mm thick PMMA resist is patterned to a depth of more than 200 μm. The resist pattern shown in Fig. 2.8 is 230 μm thick and exhibits a 2 μm gap between the inner cylinder and the pickup electrodes (aspect ratio is 100:1). The resonator pattern was produced using soft (1 nm length) x- rays and a 3 μm thick Au absorber only.

Forming of the transfer mask directly on the sample surface creates several additional new opportunities; besides *in situ* development, etching, and deposition, these include exposure of samples with curved surfaces and dynamic deformation of a sample surface during the exposure (hemispherical structures for lenses are possible this way). The authors summarize the advantages of the transfer mask method as follows:

- Alleviates the difficulty in fabricating fragile mask membranes;
- Avoids alignment requirements during successive exposure steps;
- Reduces exposure time and absorber thickness for the same exposure source;
- Enhances pattern transfer fidelity, since there is almost no proximity gap;

- Avoids thermal deformation caused by exposure heat;
- Increases photoresist development rate by step-wise elevated exposure dose.

2.4.9 Choice of Resist Substrate

In the x- ray lithography process, the primary substrate, or base plate, must be a conductor or an insulator coated with a conductive top layer. A conductor is required for subsequent electrodeposition. Some examples of primary substrates that have been used successfully are Al, austenite steel plate, Si wafers with a thin Ti or Ag/Cr top layer, and copper plated with gold, titanium, or nickel.

Other metal substrates as well as metal-plated ceramic, plastic, and glass plates have been employed. It is important that the plating base provide good adhesion for the resist. For that purpose, prior to applying the x- ray resist on copper or steel, the surface sometimes is mechanically roughened by micro grinding with corundum or other abrasive media.

During chemical preconditioning, a titanium layer, sputter-deposited onto the polished metal base plate (e.g., a Cu plate), is oxidized for a few minutes in a solution of 0.5 M NaOH and 0.2 M H_2O_2 at 65 ^oC. The oxide produced typically measures 30 nm thick and exhibits a micro rough surface instrumental to securing resist to the base plate. The Ti adhesion layer may further be covered with a thin nickel seed layer (~15 nm) for electroless or electroplating of nickel. When using a highly polished Si surface, adhesion promoters need to be added to the resist. A substrate of special interest is a processed silicon wafer with integrated circuits. Integrating the x-ray lithography process with semiconductor circuitry on the same wafer will create additional x- ray lithographic applications. The rear surface of electrodeposited micro devices is attached to the primary substrate but can be removed from the substrate if required. In the latter case, the substrate may be treated chemically, or electrochemically, to intentionally induce poor adhesion. Ideally, excellent adhesion exists between substrate and resist, and poor adhesion exists between the electroplated structure and the plating base. Achieving these two contradictory demands is one of the main challenges in x- ray lithography.

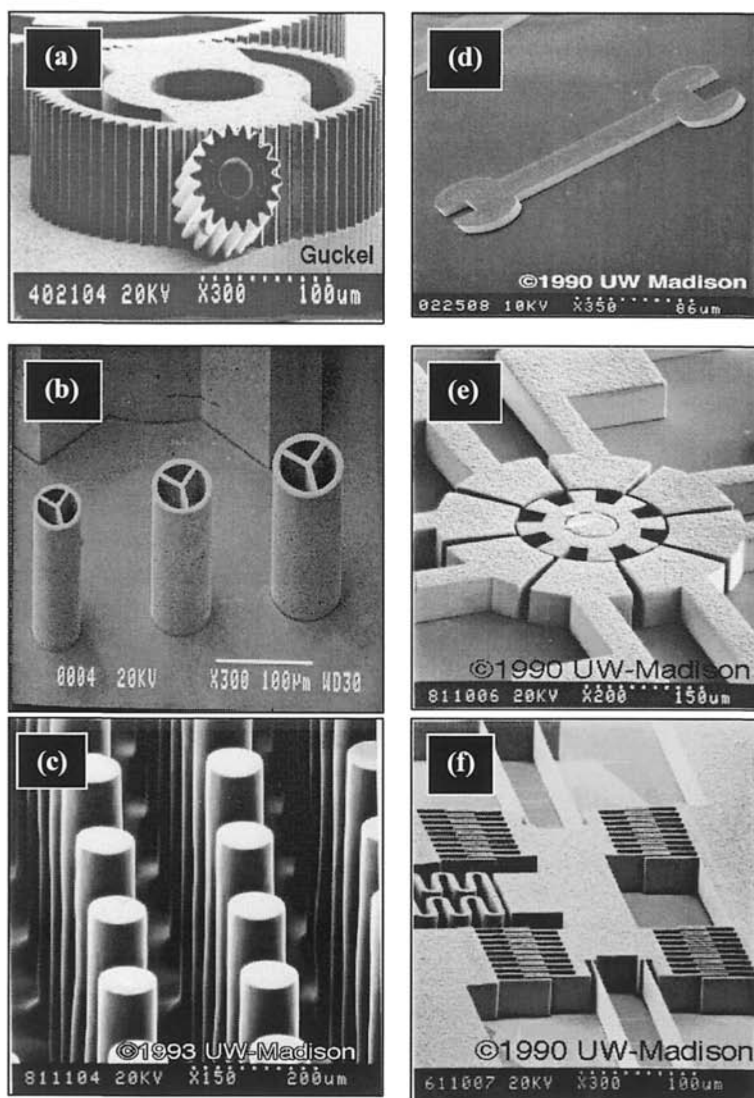

Fig. 2.8. SEM micrographs of microstructures made by the transfer mask method and multiple exposure/development steps: (a) gear and mechanism; (b) hollow pillars; (c) high aspect ratio pillars; (d) wrench; (e) metering device; and (f) comb drive (Courtesy of the University of Wisconsin at Madison)

2.4.10 Resist Requirements

An x- ray resist ideally should have high sensitivity to x- rays, high resolution, resistance to dry and wet etching, thermal stability of greater than 140 ^{O}C, and a matrix or resin absorption of less than 0.35 μm^{-1} at the wavelength of interest. These requirements are only those for semiconductor production with x- ray lithography. To produce high-aspect-ratio microstructures with high lateral tolerances an additional set of requirements is required. The unexposed resist must be absolutely insoluble during development. This means that a high contrast (γ) is required. The resist must also exhibit very good adhesion to the substrate and be compatible with the electroforming process. The latter imposes a resist glass transition temperature (T_g) greater than the temperature of the electrolyte bath used to electrodeposit metals between the resist features remaining after development (say, at 60 ^{O}C). To avoid mechanical damage to the microstructures induced by stress during development, the resist layers should exhibit low internal stresses. If the resist structure is the end product of the fabrication process, further specifications depend on the application itself, for example, optical transparency and refractive index for optical components or large mechanical yield strength for load-bearing applications. Owing to excellent contrast and good process stability known from electron beam lithography, PMMA is the preferred resist for deep-etch synchrotron radiation lithography. Two major concerns with PMMA as the x- ray lithography resist are a rather low lithographic sensitivity of about 2 J/cm^2 at a wavelength λ_c of 0.84 nm and a susceptibility to stress cracking. For example, even at shorter wavelengths, $\lambda_c = 0.5$ nm, over 90 min of irradiation are required to structure a 500 μm thick resist layer with an average ring storage current of 40 mA and a power consumption of 2 MW at the 2.3-GeV ELSA synchrotron. The internal stress arising from the combination of a polymer and a metallic substrate can cause cracking in the microstructures during development, a phenomenon PMMA is especially prone to. X- ray resists explored for lithographic applications include poly(lactides), for example, poly(lactide-co-glycolide) (PLG); polymethacrylimide (PMI); polyoxymethylene (POM); and polyalkensulfone (PAS). PLG is a new positive resist that is more sensitive to x- rays by a

factor of 2 to 3 compared with PMMA. From the comparison of different resists for deep x- ray lithography in Table 2.4, PLG emerges as the most promising x- ray lithography resist. POM, a promising mechanical material, may also be suited for medical applications given its biocompatibility. All of the resists shown in Table 2.6 exhibit significantly enhanced sensitivity compared to PMMA, and most exhibit reduced stress corrosion. Negative x- ray resists have inherently higher sensitivities compared to positive x- ray resists, although their resolution is limited by swelling. Poly(glycidyl methacrylate-co-ethyl acrylate) (PGMA), a negative electron beam resist has also been used in x- ray lithography. In general, resist materials sensitive to electron beam exposure also display sensitivity to x- rays and function in the same fashion; materials positive in tone for electron beam radiation typically are also positive in tone for x-ray radiation. A strong correlation exists between the resist sensitivities observed with these two radiation sources, suggesting that the reaction mechanisms might be similar for both types of irradiation. More common x- ray resists from the semiconductor industry are reviewed in Table 2.5.

Table 2.4. Properties of resists for deep x- ray lithography

Feature	PMMA	POM	PAS	PMI	PLG
Sensitivity	-	+	++	0	0
Resolution	++	0	--	+	++
Sidewall smoothness	++	--	--	+	++
Stress corrosion	-	++	+	-	+
Adhesion on substrate	+	+	+	-	+

Note: PMMA = poly(methylmethacrylate), POM = polyoxymethylene, PAS = Polyalkensulfone, PMI = polymethacrylimide, PLG = poly(lactide-co-glycolide). ++ = excellent; + = good; 0 = reasonable; - = bad; -- = very bad.

2.5 Methods of Resist Application

2.5.1 Multiple Spin Coats

Different methods to apply ultra thick layers of PMMA have been studied. In the case of multi-layer spin coating, high interfacial stresses between the layers can lead to extensive crack propagation upon developing the exposed resist.

Table 2.5. Resist materials used for electron beam and x- ray lithography processes.

Novolak-based resist	EBL sensitivity ($\mu C/cm^2$)	EBL contrast	XRL sensitivity (mJ/cm^2)	XRL contrast
PMMA	100	2.0	6500	2.0
PBS	1	2.0	170	1.3
EBR-9	1.2	3.0		
Ray-PF			125	*
COP	0.5	0.8	100	1.1
GMCIA	7.0	1.7		
DCOPA			14	1.0
Novolak based	200-500	2-3	750-2000	~

*Indicates that the value is process dependent.

2.5.2 Commercial PMMA Sheets

High molecular weight PMMA is commercially available as prefabricated plate and several groups have employed freestanding or bonded PMMA resist sheets for producing x- ray lithography structures. After overcoming the initial problems encountered when attempting to glue PMMA foils to a metallic base plate with adhesives, this has become the preferred method in several laboratories.

2.5.3 Casting of PMMA

PMMA also can be purchased in the form of a casting resin. In a typical procedure, PMMA is *in situ* polymerized from a solution of 35 wt% PMMA of a mean molecular weight of anywhere from 100,000 g/mol up to 10^6 g/mol in methylmethacrylate (MMA). Polymerization at room temperature takes place with benzoyl peroxide (BPO) catalyst as the hardener (radical builder) and dimethylaniline (DMA) as the initiator. The oxygen content in the resin, inhibiting polymerization, and gas bubbles, inducing mechanical defects, are reduced by degassing while mixing the components in a vacuum chamber at room temperature and at a pressure of 100 mbar for 2 to 3 min. In a practical application, resin is dispensed on a base plate provided with shims to define pattern and thickness and subsequently covered with a glass plate to avoid oxygen absorption.

2.5.4 Resist Adhesion

Smooth surfaces such as Si wafers with an average roughness, R_a, smaller than 20 nm pose additional adhesion challenges that are often solved by modifying the resist itself. To promote adhesion of resist to polished untreated surfaces, such as a metal-coated Si wafers, coupling agents must be used to chemically attach the resist to the substrate. An example of such a coupling agent is methacryloxypropyl trimethoxy silane (MEMO). With 1 wt% of MEMO added to the casting resin, excellent adhesion results. The adherence is brought about by a siloxane bond between the silane and the hydrolyzed oxide layer of the metal. The integration of this coupling agent in the polymer matrix is achieved via the double bond of the

methacryl group of MEMO. Hydroxyethyl methacrylate (HEMA) can improve PMMA adhesion to smooth surfaces, but higher concentrations are needed to obtain the same adhesion improvement. Silanization of polished surfaces prior to PMMA casting, instead of adding adhesion promoters to the resin, did not seem to improve the PMMA adhesion. In the case of PMMA sheets, as mentioned before, one option is solvent bonding of the layers to a substrate. In another approach, Galhotra et al. [40] mechanically clamped the exposed and developed self-supporting PMMA sheet onto a 1.0 mm thick Ni sheet for subsequent Ni plating.

2.5.5 Stress-Induced Cracks in PMMA

The internal stress arising from the combination of a polymer on a metallic substrate can cause cracking in the microstructures during development. To reduce the number of stress-induced cracks, both the PMMA resist and the development process must be optimized. Detailed measurements of the heat of reaction, the thermomechanical properties, the residual monomer content, and the molecular weight distribution during polymerization and soft baking have shown the necessity to produce resist layers with a high molecular weight and with only a very small residual monomer content.

2.6. Exposure

2.6.1 Optimal Wavelength

For a given polymer, the lateral dimension variation in a x- ray lithography microstructure could, in principle, result from the combined influence of several mechanisms. These include Fresnel diffraction, the range of high-energy photoelectrons generated by the x-rays, the finite divergence of synchrotron radiation, and the time evolution of the resist profiles during the development process. The theoretical results demonstrate that the effect of Fresnel diffraction (edge diffraction), which increases as the wavelength increases, and the effect of secondary electrons in PMMA, which increases as the

wavelength decreases, lead to minimal structural deviations when the characteristic wavelength ranges between 0.2 and 0.3 nm (assuming an ideal development process and no x- ray divergence). To fully utilize the accuracy potential of a 0.2 to 0.3nm wavelength, the local divergence of the synchrotron radiation at the sample site should be less than 0.1 mrad. Under these conditions, the variation in critical lateral dimensions likely to occur between the ends of a 500 μm high structure due to diffraction and secondary electrons is estimated to be 0.2 μm. The estimated Fresnel diffraction and secondary electron scattering effects are shown as a function of characteristic wavelength in Fig. 2.9.

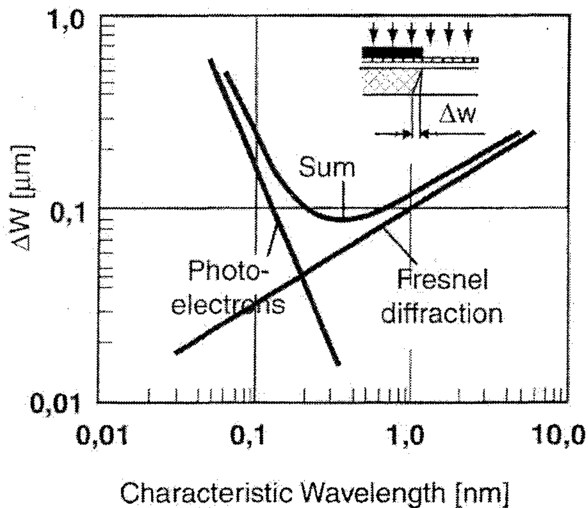

Fig. 2.9. Fresnel diffraction and photoelectron generation as a function of characteristic wavelength, λ_c, and the resulting lateral dimension variation (ΔW). (From W. Menz and P. Bley, "Microsystems for Engineers", VCH Publishers, Germany, 1993)

Using cross-linked PMMA, or linear PMMA with a unimodal and extremely high molecular weight distribution (peak molecular weight greater than 1,000,000 g/mol), the experimentally determined lateral tolerances on a test structure as shown in Fig. 2.10 are 55 nm

per 100 μm resist thickness, in good agreement with the 0.2 μm over 500 μm expected on a theoretical basis. These results are obtained only when a resist/developer system with a ratio of the dissolution rates in the exposed and unexposed areas of approximately 1000 is used. The use of resist layers, not cross-linked and displaying a relatively low bimodal molecular weight distribution, as well as the application of excessively strong solvents such as used to develop thin PMMA resist layers in the semiconductor industry, lead to more pronounced conical shape in the test structure of Fig. 2.10. An illustration of the effect of molecular weight distribution on lateral geometric tolerances is that linear PMMA with a peak molecular weight below 300,000 g/mol shows structure tolerances of up to 0.15 μm/100 μm. To obtain the best tolerances requires a PMMA with a very high molecular weight, also a pre-requisite for low stress in the developed resist. Finally, if the synchrotron beam is not parallel to the absorber wall but at an angle greater than 50 mrad, greater angles may result.

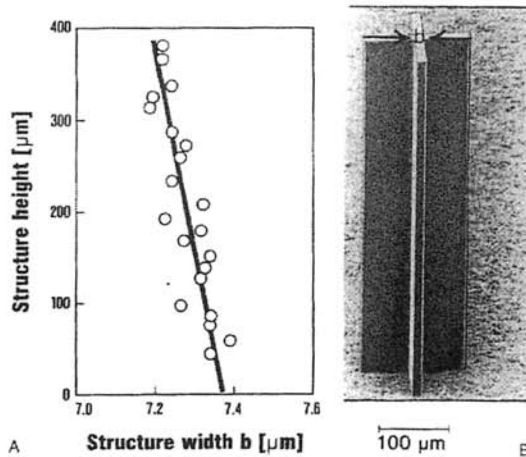

Fig. 2.10. Structural tolerances. (A) SEM micrograph of a test structure to determine conical shape. (B) Structural dimensions as a function of structure height. The tolerances of the dimensions are within 0.2 μm over the total structure height of 400 μm (From J. Mohr, W. Ehrfeld, and D. Munchmeyer, in J. Vac. Sci. Technol., Volume B6, 1988, p.p. 2264-2267)

2.6.2 Deposited Dose

The x- ray irradiation of PMMA reduces the average molecular weight. For one-component positive resists, this lowering of the average molecular weight causes the solubility of the resist in the developer to increase dramatically. The average molecular weight making dissolution possible is a sensitive function of the type of developer used and the development temperature. The molecular weight distribution, measured after resist exposure, is unimodal with peak molecular weights ranging from 3000 g/mol to 18,000 g/mol, dependent on the dose deposited during irradiation.

The peak molecular weight increases nearly linearly with increasing resist depth; that is, decrease of the absorbed dose. Fig. 2.11A illustrates a typical bimodal molecular weight distribution of PMMA before radiation, exhibiting an average molecular weight of 600,000. The gray region in this figure indicates the molecular weight region where PMMA readily dissolves; that is, below the 20,000 g/mol level for the temperature and developer used.

Since the fraction of PMMA with a 20,000 molecular weight is very small in non-irradiated PMMA, the developer hardly attacks the resist at all. After irradiation with a dose D_{dv} of 4 kJ/cm^3, the average molecular weight becomes low enough to dissolve almost all of the resist (Fig. 2.11B). With a dose D_{dm} of 20 kJ/cm^3, all of the PMMA dissolves swiftly (Fig. 2.11C). At a dose above D_{dm}, the microstructures are destroyed by the formation of bubbles. It follows that to dissolve PMMA completely and to make defect-free microstructures, the radiation dose for the specific type of PMMA used must lie between 4 and 20 kJ/cm^3.

These two numbers also lock in a maximum value of 5 for the ratio of the radiation dose at the top and bottom of a PMMA structure. To make this ratio as small as possible, the soft portion of the synchrotron radiation spectrum is usually filtered out by a pre-absorber (for example, a 100 μm thick polyimide foil [Kapton]) to reduce differences in dose deposition in the resist.

2.6.3 Stepped and Slanted Microstructures

For many applications, stepped or inclined resist sidewalls are very useful – consider, for instance, the fabrication of multi-level devices or prisms or, more basic yet, angled resist walls to facilitate the release of molded parts. Using stepped absorber layers on a single mask to make stepped multilevel microstructures is not always very well resolved.

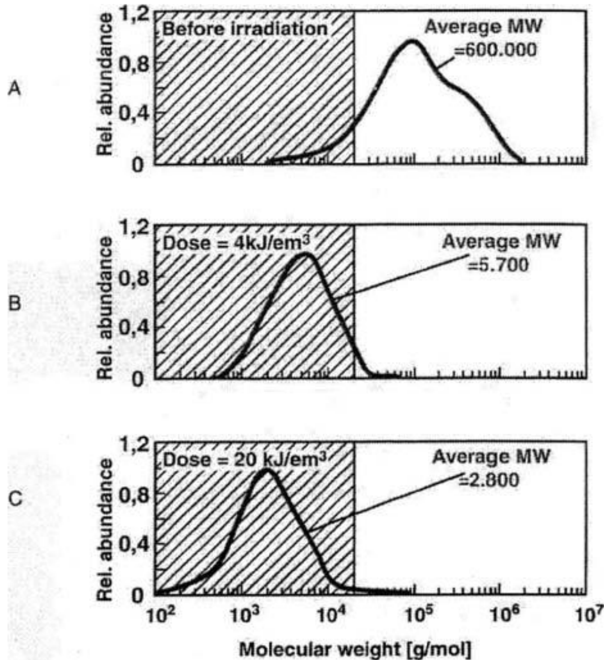

Fig. 2.11. Molecular weight distribution of PMMA before (A) and after irradiation with 4 (B) to 20 kJ/cm^3 (C). The shaded areas indicate the domain in which PMMA is minimally 50% dissolved (From W. Menz and P. Bley, "Microsystems for Engineers", VCH Publishers, Germany, 1993)

To make better-resolved stepped features, one can first relief print a PMMA layer, for example, by using a Ni mold insert made

from a first x- ray mask. Subsequently, the relief structure may be exposed to synchrotron radiation to further pattern the polymer layer through a precisely adjusted second x- ray mask. To carry out this process, a two-layer resist system needs to be developed consisting of a top PMMA layer that fulfills the requirement of the relief printing process, and a bottom layer that fulfills the requirements for x-ray lithography. The bottom resist layer promotes high molecular weight and adhesion, while the top PMMA layer is of lower molecular weight and contains an internal mold-release agent. This process sequence, combining plastic impression molding with x- ray lithography, is illustrated in Fig. 2.12. The two-step resist then facilitates the fabrication of a mold insert by electroforming, which can be used for the molding of two-step plastic structures. Extremely large structural heights can be obtained from the additive nature of the individual microstructure levels. There are several options for achieving miniaturized features with slanted walls. It is possible to modulate the exposure/development times of the resist, fabricate an inclined absorber, angle the radiation, or, move the mask during exposure in so-called moving mask deep x- ray lithography.

To make a slanted absorber, a slab of material can be etched into a wedge by pulling it at a linear rate out of an etchant bath. Changing the angle at which synchrotron radiation is incident upon the resist, usually 90 degrees, also enables the fabrication of microstructures with inclined sidewalls. This way, slanted microstructures may be produced by a single oblique irradiation or by a swivel irradiation. One potentially very important application of microstructures incorporating inclined sidewalls is the vertical coupling of light into waveguide structures using a 45 degree prism. Such optical devices must have a wall roughness of less than 50 nm, making x- ray lithography a preferred technique for this application. The sharp decrease of the dose in the resist underneath the edge of the inclined absorber, and the resulting sharp decrease of the dissolution of the resist as a function of the molecular weight in the developer, results in little or no deviation of the inclination of the resist sidewall over the total height of the microstructure.

2.6.4 Master Micromold Fabrication Methods

The high cost of x- ray lithography has required that engineers search for alternative means of fabricating high-aspect ratio metal or polymer micromasters. Micromold inserts (or micromasters) can be fabricated by a variety of alternate techniques such as CNC machining, silicon wet bulk micromachining, precision EDM, thick deep UV resists, DRIE, excimer layer ablation, and electron beam writing. In Table 2.6, x- ray lithography metal molds are compared with metal masters fabricated by other means.

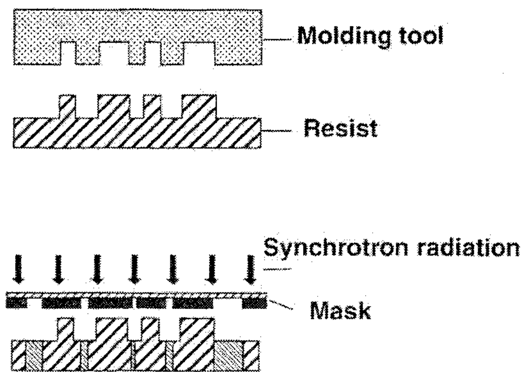

Fig. 2.12. Stepped microstructures made in the x- ray lithography process (From W. Menz and P. Bley, "Microsystems for Engineers", VCH Publishers, Germany, 1993)

For example, comparing metal mold inserts made by spark erosive cutting and x- ray lithography, the latter proves far superior. X-ray lithographic PMMA features as small as 0.1 μm are replicated in the metal shape with almost no defects. The electroformed structures have a superior surface quality with a surface roughness, R_a, of less than 0.02 μm.

DRIE and thick deep UV-sensitive resists such as polyimides, are recent contenders for micromaster mold fabrication. With respect to dry etching, higher and higher aspect ratio features are being achieved, especially when using highly anisotropic etching conditions as in cryogenic DRIE. Wall roughness, causing form locking,

remains a problem with DRIE; the dry etching process was optimized for speed, not for demolding. For small-quantity production, where the lifetime of mold inserts is not crucial, a silicon wafer etched by DRIE can be utilized directly as a mold insert for anywhere from 5 to 30 molding cycles.

For longer-lasting molds, metallizing the Si structure and using the metal as the mold is preferred. Photoresist structures on a silicon substrate have also been tested as a mold insert in plastic molding because of the simplicity and low cost of the process. In low-pressure molding processes, such mold inserts do work for a limited number of production processes (applying a thin metal layer over the top of the resist may further extend the lifetime of the mold), but their applicability in high-pressure processes needs to be further verified.

Table 2.6. Comparison of micromolds manufactured using a variety of techniques.

Parameter	Laser	CNC machining	Electro discharge machining	X- ray lithography	Deep ultra violet	Deep reactive ion etching
Aspect Ratio	<10	14	<100	100	22	10-25
Roughness	100nm - 1 μm	3-5 μm	0.3 - 1 μm	<20 nm	1 μm	2 μm
Accuracy	3-5 μm	3-5 μm	1-3 μm	<1 μm	2-3 μm	<1 μm
Maximum Height	300 μm	Unlimited	3-5 mm	<10mm	300 μm	300 μm
Mask Required?	No	No	No	Yes	Yes	Yes

Both DUV and DRIE are more accessible than x- ray lithography and will continue to improve, taking more opportunities away from x- ray lithography. Like x- ray lithography, both alternative techniques can be coupled with plating, but neither technique can yet achieve the extreme low surface roughness and vertical walls of x-

ray lithography. Other competing technologies for making metal masters are laser ablation methods and ultra-precision CNC machining. The latter three methods are serial processes and rather slow, but since we are considering the production of a master only, these technologies might well be competitive for certain applications.

Laser microablation produces minimum features of about 10 μm width and aspect ratios of 1:10. Challenges include taper and surface finish control. Recast layers around the laser-drilled features cause form locking and infidelity in the replication. Femtosecond pulse layers promise thinner or even the absence of recast layers and excellent resolution. For large features (>50 μm) with tolerances and repeatability in the range of about 10 μm, traditional CNC-machining of materials like tool steel and stainless steel is often accurate enough for making metal mold inserts. The advantage of this technique is that the tool materials used are the same as those in conventional polymer molding, so their design, strength, and service life are well established. Complicated 3D structures can also be machined easily. The main disadvantages are that it is difficult to make sharp corners or right angles, and the surface quality is usually poor (surface roughness is around several micrometers). In contrast, lithographic methods can produce molds with excellent surface quality (surface quality < 0.1 μm) and sharp corners or right angles. However, they cannot be used on conventional tool materials such as steel. Diamond-based micromilling and microdrilling reduce the surface roughness to 1 μm or less. While diamond-based methods can achieve features smaller than 10 μm, they are applicable only to "soft" metals such as nickel, aluminum, and copper.

As shown in Table 2.6, a significant potential application of x-ray lithography remains the fabrication of those metal molds that cannot be accomplished with other techniques because of the tight wall roughness tolerances, small size, and high aspect ratios. From the table, it is obvious that x- ray lithography micromolds are extremely well suited at very low surface roughness levels and in terms of accuracy.

Summarizing, the requirements for an optimal mold insert fabrication technique are as follows:

- The master has to be removed from the molded structure, so the ease of release through wall inclination control is crucial;
- The most important parameters, including master life and achievable aspect ratios, depend very strongly on the surface quality of the master;
- The interface chemistry between master and polymer is a critical factor and must be controlled.

2.6.5 Future Directions

The full potential of microfabrication using x- ray lithography and the LIGA technique has yet to be realized. Advances in process technology, a greater understanding of the physics of x- ray interactions in resist materials and the availability of more intense, higher energy beams from synchrotrons provide some solutions to earlier problems and new opportunities for industrial and commercial exploitation. The future value of the technique resides in its ability to mass-produce at low cost, precision microcomponents that cannot be made using other processes. This requires design rules and agreed standards in processing and manufacturing.

Most of the technical and process knowledge exists in research centers that have links or access to synchrotron sources. The limitation in the range of materials that can be electroformed preclude many application areas. This is, however, offset by the growth in polymer and ceramic components required in almost all sectors of industry and, in particular, medical diagnostics, chemical analysis, environmental sensors, optical displays, and communications. The technology fits into the tool-making industry as basically precision molds and parts are used in the production process. The tool-making industry has an annual turnover of $90 billion, and with a rapid growth rate predicted over the next 5 years it provides an ideal market sector for the technology.

Unfortunately there has been very little technology transfer into industry with only a few spin-off companies providing services and a limited number of products. In common with many non-IC-based

technologies, industry has not been convinced that LIGA has reached a level of maturity and a potential to mass-produce components that are free of defects and have total reliability. The high cost and accessibility to synchrotrons, the only suitable source of x- rays, is one of the barriers to wider use of the technique. Germany saw future opportunities and in 1997 built and opened ANKA, 2.5 Gev Synchrotron facility with three dedicated lithography beam lines. It provides, through a marketing subsidiary ANKA GmbH, a full range of analytical and manufacturing services on a commercial basis.

Many countries in the Asia–Pacific rim are now looking at non-silicon-based microfabrication technologies and have large growing markets for products. China, Taiwan, Korea, Singapore, have synchrotrons and microfabrication manufacturing facilities. They all are members of the global MEMS community and are adding to the research and development targeted toward the realization of commercial products. It is therefore likely that many of the problems mentioned above will be solved in the foreseeable future.

The recent establishment of an international LIGA Interest Group to bring together groups around the word and to act as a driver for commercialization is supported by Germany's FZK and the Sandia National Laboratories at Livermore, and the Center for Advanced Microstructures and Devices (CAMD) at the Louisiana State University at Baton Rouge, in the United States. This is a step towards making sure that all the work that has been carried out during the last sixteen years will be directed towards providing useful products.

2.7 Problems

1. What is x- ray lithography?
2. Explain the principles associated with synchrotron radiation.
3. Explain how synchrotron radiation is used to manufacture micro components and systems.
4. Describe the spectral characteristics of deep x- ray lithography.
5. Describe the LiGA process.

6. What are x- ray masks?
7. Compare masks used in x- ray lithography and the semiconductors industry.
8. Describe the materials used for masks.
9. Explain how masks are made for use when machining high aspect ratio microlithographic components.
10. How do you choose a suitable resist for the substrate material?
11. What are the requirements of a resist material?
12. Explain how resists are applied to substrates.
13. Explain the many ways to manufacture master molds.
14. Show how gears, mechanisms, metering devices, and comb drives are produced using deep x- ray lithography.

References

1. Ehrfeld W, Becker EW, Hagmann P, Maner P and Munchmeyer P, Microelectron. Engin., 1986, **4**, pp 35-56.
2. Bacher W et al., IEE Transac. Industrial Electron, **42** (5), 1995.
3. Hruby, J (Ed), Goettert , J. Proceedings HARMST 2003, Monterey, June 2003.
4. Tolfree DWL, Proceedings of COMS2003, Amsterdam, Netherlands, Sept 2003.
5. Goettert, J., Proceedings of COMS2004, Edmonton, Canada, Sept 2004.
6. NEXUS 'Market Analysis for Microsystems 2000-2005, Feb 2002.
7. Madou M, 'Fundamentals of Microfabrication', 2nd Edition, 2002, CRC Press).
8. Tolfree DWL, Microfabrication using Synchrotron Radiation, Progress Reports in Physics, **61**, 4, 1998.
9. Cerrina F, Handbook on Lithography, SPIE edition, 1996
10. Becker E, Betz H, Ehrfeld W, Glashauser W, Michael H, Munchmeyer D, Pongratz S and Von Siemens R, 1982, Naturwissenschaften, **69,** 520-523.
11. Ehrfeld W, Becker E W, Hagmann P, Maner P and Munchmeyer P, Microelectron. Engin., 1986, **4,** 35-56.
12. Ehrfeld W, Bley P, Gotz F, Hagmann P, Mane A, Mohr J and Herbert O, 1987, Proc IEEE Micro robots and Teleoperators Workshop (Fabrication of Microstructures using the LIGA process), **87,** 1-11.

13. Ehrfeld W, Bley P, Gotz J, Munchmeyer D, Mohr J, Schulb W, 1988, J Vac. Sci. **B6**.
14. Ehrfeld W and Lehr H, 1994, Journal de Physique, **4**, p C9-229-236.
15. Ehrfeld W and Lehr H, 1995, Rad. Phys & Chem., **45,** pp 349-365.
16. Bley P, Gottert, Haemening M, Himmelhaus M, Menz W, Mohr J, Muller C and Wallrabe U, 1991, Microsystem Technologies 1991 (ed H Reichl), 302-314, Heidelberg, Springer-Verlag.
17. Bley P, 1993, Interdisciplinary Science Reviews, **18**, 3, p. 267.
18. Harmening M, Bacher W, Bley P, El-Kholi, Kalb H, Kowanz, Menz, Michel A and Mohr J., 1992, MEMS, No. 0-7803-0497-7/92. 202-207, New York IEEE.
19. Tolfree D and Ehrfeld W, 1994, Proc. Tech. Trans.Conf,, Published by TCD.
20. Bacher W, Menz W and Mohr J, 1995, IEE Trans. on Industrial Elect. Vol. 42.
21. Guckel H, Skrobis K, Christenson T, Klein J, Han, Choi B, Loverell E and Chapman T, 1991, Proc. Transducers (San Francisco) (New York : IEEE).
22. Guckel H, 1993, N. I. M. in Physics Res, Section B, **B79**, 1-4, pp 247-8.
23. Guckel H, Skrobis K, Christenson T and Klein J, 1994, SPIE's Symposium on Microlithography, p.p. 2194-09.
24. Guckel H and Christenson T R, 1995, SPIE Meeting, Oct. 1995, Austin, Texas.
25. Tomboulian DH and Hatman, 1956, Phys. Rev. **102,** 1423-47.
26. Sokolov AA and Ternov IM, 1957, Sov. Phys., JETP, **4,** 396-400.
27. Sokolov AA and Ternov IM, 1968, Synchrotron Radiation, (Berlin : Academie- Verlag).
28. Godwin RP 1969, Synchrotron Radiation as a Light Source, (Springer Tracts in Modern Physics 51, ed. J. Hohler.
29. Rowe EM, 1979, Synchrotron Radiation (topics in Current Physics 10), ed. C. Kunz, (Berlin Springer), pp 25-54.
30. Winick H, 1980, Synchroton Radiation Research, ed. Winick and Doniach (New York: Plenum), p.p. 11-60.
31. Grobman W, 1985, Synchrotron Radiation Research, Winick H ed. Pergamon, N.Y.
32. Ternov IM, Mikhailin VV and Khalilov VR, 1985, Synchrotron Radiation and its Applications (New York: Harwood).
33. Marks N, 1995, Radiat. Phys. Chem., **45**, 3, pp 315-331.

34. Turner S, 1989, Synchrotron Radiation and Free Electron Lasers, CERN Acc. School, Chester, Cern 90-30.
35. Krinsky S, Perlman M L and Watson R E, 1993, Handbook on Synchrotron Radiation, E Koch ed., North Holland, pp. 65-172.
36. Tomboulian D H and Hatman, 1956, Phys. Rev., **102,** 1423-47.
37. Timothy JG and Madden R P, 1983, Handbook on Synchrotron Radiation, Vol 1A, editor E E Koch (Amersterdam: North-Holland), pp325-66.
38. Elleaume P, 1990, Phys. Scripta, **T31,** 67-71.
39. Yamamonto S, Shio T, Sasaki S and Kitamura H, 1989, Rev Sci. Instrum., **60,** 1834-7.
40. Galhotra V, Marques C, Desta Y, Kelly K, Despa M, Pendse A, and Collier A., in Proceedings of the SPIE: Micromachining nd Microfabrication Process Technology II, Austin, TX, 1996, p.p. 168-173.